Proceedings of the Sixteenth International Conference on
Computational Structures Technology
Edited by: P. Iványi, J. Kruis and B.H.V. Topping
Civil-Comp Conferences, Volume 14, Paper 5.1
Civil-Comp Press, Edinburgh, United Kingdom, 2026
ISSN: 2753-3239, doi: 10.4203/ccc.14.5.1

Surrogate Modeling for a Multi-Species Biofilm Model

H. Geisler, F. Klempt, M. Soleimani and P. Junker

Institute of Continuum Mechanics, Leibniz University Hannover, Germany

Abstract

The study of biomechanics not only helps in understanding the fundamental principles governing biological systems but also plays a crucial role in the development of medical treatments, rehabilitation strategies, and the design of biomimetic materials. Unfortunately, the complexity of biological systems often leads to computationally expensive nonlinear models, which can be a significant barrier to their practical application. In this contribution, we assess the Time-separated Stochastic Mechanics (TSM) as a surrogate modeling approach aimed at mitigating the computational demands of a recently developed multi-species biofilm model. The model is able to capture the complex interactions between different bacterial species within a biofilm, including competition for resources and the effects of antibiotics.

Keywords: biofilm modeling, multi-species interaction, Time-separated Stochastic Mechanics

1 Introduction

Biofilms are occurring ubiquitously across nature, medicine and industry. Examples include the diverse microflora of the human gut or the dental plaque or wastewa-

ter treatment bioreactors. The vast majority of biofilm-related phenomena are multi-species in nature [3, 4].

The internal dynamics of these multi-species films are governed by a variety of biological and chemical interactions. The individual species within the biofilm do not exist in isolation but engage in constant competition for space and nutrients. Furthermore, they can engage in synergetic relationships where the metabolic byproduct of one species becomes an energy source for another [5, 6].

In order to predict the growth and evolution of such complex systems, robust mathematical models are needed. In vitro experiments provide critical raw data but are intrinsically time consuming and expensive. Computer-assisted in silico experiments offer a powerful alternative, allowing to explore the dynamics of multi-species films under a wide range of environmental conditions and to optimize treatments against harmful biofilms [7].

Unfortunately, the complexity of the underlying biological processes often leads to computationally expensive nonlinear models, which can be a significant barrier to their practical application. In particular, the evaluation of such models for a wide range of parameters, e.g., different antibiotic dosages and timings, can become computationally prohibitive when it needs to be evaluated many times. Therefore, different surrogate modeling approaches have been developed to mitigate the computational demands of complex models. These surrogate models are simplified versions of the original model that are computationally much cheaper to evaluate. In this work, we evaluate the Time-separated stochastic mechanics as a surrogate model for a recently proposed biofilm model.

2 Biofilm model

In this section, the biofilm model as presented in [1] is recalled. A biofilm is composed of n different bacterial species that grow and interact with each other. Each species i is characterized by its volume fraction $\phi_i \in [0, 1]$. The volume fraction indicates the portion of the total volume available for growth that is occupied by species i. The remaining free volume is empty space ϕ_0. We collect all volume fractions in the vector

$$\boldsymbol{\phi} = [\phi_0, \phi_1, \phi_2, \ldots, \phi_n]^T . \tag{1}$$

The total volume of all bacteria plus the empty space is bounded by the available volume, i.e.,

$$f := \sum_{i=0}^{n} \phi_i - 1 = 0 \tag{2}$$

In order to model the death of biofilm, a second internal state variable is introduced. The fraction of living bacteria of species i is given as $\psi_i \in [0, 1]$. The vector of all fractions of living bacteria is given as

$$\boldsymbol{\psi} = [\psi_1, \psi_2, \ldots, \psi_n]^T . \tag{3}$$

Consequently, the volume occupied by living bacteria of species i is given as $\bar{\phi}_i = \phi_i \, \psi_i \; \forall i$ or equivalently as a vector as

$$\bar{\boldsymbol{\phi}} = \left[\phi_1\psi_1, \; \phi_2\psi_2, \ldots, \phi_n\psi_n\right]^T \tag{4}$$

Thus, the complete vector of internal state variables is given as $\boldsymbol{\xi} = (\boldsymbol{\phi}, \boldsymbol{\psi})^T$

In order to derive a mathematical model for the evolution of the internal state variables, we use Hamilton principle of stationary action [8]. The principle has found various applications in continuum mechanics, due to the automatic fulfillment of the first and second law of thermodynamics. The model is derived from a potential that consists of three parts: the free energy, the dissipation potential and possibly constraint potentials.

Hamilton's principle for a quasi-static and isothermal process is given as

$$\mathcal{H} = \int_\tau (\mathcal{G} + \mathcal{C} + \mathcal{D}) \, \mathrm{d}t \rightarrow \underset{\boldsymbol{\xi},\gamma}{\operatorname{stat}} \tag{5}$$

with the free energy functional $\mathcal{G}$, the constraint functional $\mathcal{C}$ and the dissipation functional $\mathcal{D}$. Requiring stationarity of the Hamiltonian with respect to the internal state variables $\boldsymbol{\xi}$ and the Lagrange multiplier γ yields the evolution equations for the internal state variables and the constraint equation, respectively.

The total potential is given as

$$\mathcal{G} = \int_\Omega \Psi + \Psi_{\text{penalty}} \, \mathrm{d}V \tag{6}$$

with the Helmholtz free energy density Ψ and the penalty energy density Ψ_{penalty}. For the free energy density we choose

$$\Psi = -\frac{1}{2} c^* \, \bar{\boldsymbol{\phi}} \cdot \boldsymbol{A} \cdot \bar{\boldsymbol{\phi}} + \frac{1}{2} \alpha^* \boldsymbol{\psi} \cdot \boldsymbol{B} \cdot \boldsymbol{\psi} \tag{7}$$

with the symmetric growth coefficient matrix $\boldsymbol{A}$ and the antibiotic sensitivity matrix $\boldsymbol{B} = \operatorname{diag}(b_1, b_2, \ldots, b_n)$. This potential is motivated by the observation that the growth of biofilm is driven by the nutrients c^*, whereas the antibiotics α^* lead to the death of biofilm. The off-diagonal entries of $\boldsymbol{A}$ model the interaction between different species, i.e., competition or symbiosis. A positive entry a_{ij} indicates that species i supports the growth of species j, whereas a negative entry indicates that species i inhibits the growth of species j. The big advantage of this approach is that the interaction between an arbitrary number of species can be modeled without introducing additional state variables.

In order to ensure that the volume fractions ϕ_i and ψ_i remain in the interval $[0, 1]$, a barrier method [9, Ch. 6.3] is used. The barrier method acts as an artificial energy that penalizes the volume fractions as they approach the extremes of 0 and 1. The penalty energy density is given as

$$\Psi_{\text{penalty}} = \frac{K_0}{\phi_0^2(1-\phi_0)^2} + \sum_{i=1}^{n} \frac{K_i}{\phi_i^2(1-\phi_i)^2} + \frac{K_i}{\psi_i^2(1-\psi_i)^2} \tag{8}$$

The dissipated energy is given as

$$\mathcal{D} = \int_\Omega \boldsymbol{p}_{\text{diss}} \cdot \boldsymbol{\xi} \, \mathrm{d}V = \int_\Omega \frac{\partial \Delta_{\text{diss}}}{\partial \dot{\boldsymbol{\xi}}} \cdot \boldsymbol{\xi} \, \mathrm{d}V \tag{9}$$

with the non-conservative dissipative forces $\boldsymbol{p}_{\text{diss}}$ and the scalar dissipation function Δ_{diss}. The non-conservative force exerts work along the internal state variables similar to the mechanical work, i.e., of traction forces $\boldsymbol{t} \cdot \boldsymbol{u}$. The specific choice for the non-conservative force allows to model path-dependent processes, as the dissipated energy and the entropy production are independent.

The dissipation energy density is modeled as

$$\Delta_{\text{diss}} = \frac{1}{2} \dot{\bar{\boldsymbol{\phi}}} \cdot \boldsymbol{\eta} \cdot \dot{\bar{\boldsymbol{\phi}}} + \frac{1}{2} \dot{\boldsymbol{\phi}} \cdot \bar{\boldsymbol{\eta}} \cdot \dot{\boldsymbol{\phi}} \tag{10}$$

with the diagonal viscosity matrix $\boldsymbol{\eta} = \text{diag}(\eta_1, \eta_2, \ldots, \eta_n)$ and $\bar{\boldsymbol{\eta}} = \text{diag}(1, \eta_1, \eta_2, \ldots, \eta_n)$. As only the living bacteria can dissipate energy due to growth processes, the dissipation is modeled in terms of the time derivative of the living bacteria volume fraction $\dot{\bar{\phi}}_i$. The second part of dissipation model ensures uniqueness of the stationary point. It should be noted that the usage of $\bar{\boldsymbol{\phi}}$ in the dissipation term leads to a coupling of the evolution equations of ϕ_i and ψ_i and complex non-linear effects arise.

The volume constraint in Equation (2) is embedded with the constraint potential

$$\mathcal{C} = \int_\Omega \gamma \left(\sum_{i=0}^{n} \phi_i - 1 \right) \mathrm{d}V \tag{11}$$

with the Lagrange multiplier γ.

2.1 Implementation

By evaluating Hamilton's principle, the strong form of the evolution equations can be derived. The evaluation of the stationarity conditions with respect to the internal state variables ϕ_i leads to

$$\begin{aligned} r_{\phi_i} := &- c^\star \psi_i \left(a_{ii} \bar{\phi}_i + \sum_{j=1}^{n-1} a_{ij} \bar{\phi}_j \right) + \eta_i (\dot{\phi}_i \psi_i^2 + \bar{\phi}_i \dot{\psi}_i + \dot{\phi}_i) \\ &- 2 \frac{K_i}{\phi_i^3 (1-\phi_i)^2} - 2 \frac{K_i}{\phi_i^2 (1-\phi_i)^3} + \gamma = 0. \end{aligned} \tag{12}$$

As special case, the stationarity condition with respect to ϕ_0 leads to

$$r_{\phi_0} := \dot{\phi}_0 + \gamma - 2 \frac{K_0}{\phi_0^3 (1-\phi_0)^2} - 2 \frac{K_0}{\phi_0^2 (1-\phi_0)^3} = 0. \tag{13}$$

Similarly, the stationarity conditions with respect to the internal state variables ψ_i yield

$$r_{\psi_i} := -c^\star \phi_i \left(a_{ii}\bar{\phi}_i + \sum_{j=1}^{n-1} a_{ij}\bar{\phi}_j \right) + \alpha^\star \psi_i b_i + \eta_i(\dot{\psi}_i \phi_i^2 + \bar{\phi}_i \dot{\phi}_i) - 2\frac{K_i}{\psi_i^3(1-\psi_i)^2} - 2\frac{K_i}{\psi_i^2(1-\psi_i)^3} + \gamma = 0. \tag{14}$$

Finally, the stationarity condition with respect to the Lagrange multiplier γ leads to

$$r_\gamma := \sum_{l=0}^{n} \phi_l - 1 = 0 \tag{15}$$

The simulation is performed on the material point level. The nutrients c^* and the antibiotics α^* are given as (time-dependent) parameters. For the time discretization an implicit Euler scheme is used. As the resulting equation system is non-linear and coupled, it is solved monolithically with a standard Newton-Raphson scheme.

3 Time-separated stochastic mechanics

For many applications, a model is evaluated not once but many times. In order to optimize the treatment of a harmful biofilm, the model needs to be evaluated for a wide range of parameters, e.g., different antibiotic dosages and timings. In model updating, the model is evaluated for different parameter sets in order to find the best fit to experimental data. In uncertainty quantification, where the model is evaluated for different parameter sets in order to quantify the uncertainty of the model predictions. For all of these applications, often hundreds or even thousands of model evaluations are needed. Even a very fast and efficient model can become computationally prohibitive when it needs to be evaluated many times. While the model at hand is comparatively computationally fast, it shares many similarities with more complex models encountered in biomechanics. In particular, a nonlinear system of equations is solved at every time step using a Newton-Raphson algorithm. This example allows us to evaluate the Time-separated stochastic mechanics (TSM) [10, 11] as a surrogate model and compare it with the reference solution.

A surrogate model is a simplified version of the original model that is computationally much cheaper to evaluate. Many surrogate models are based on a polynomial expansion of the model response in the parameter space, i.e., a Taylor expansion. The Time-separated stochastic mechanics is a novel surrogate modeling approach. The surrogate is defined by derivative matching, i.e., the first p partial derivatives of the TSM-surrogate coincide with the forward model at a given point in the parameter space. In general, the parameter space can entail many parameters, e.g., the growth coefficients a_{ij}, the antibiotic sensitivity b_i and the viscosities η_i as well as the nutrients c^* and the antibiotics α^* For a single scalar parameter θ and an evaluation point

$\theta^{(0)}$, the TSM surrogate is given as

$$\frac{\partial^i}{\partial \theta^i}\boldsymbol{\xi}(t)\big|_{\theta=\theta^{(0)}} = \frac{\partial^i}{\partial \theta^i}\boldsymbol{\xi}^{\text{TSM}}(t)\big|_{\theta=\theta^{(0)}} \quad \forall i = 0, 1, \ldots, p. \tag{16}$$

where $\boldsymbol{\xi}(t)$ are the internal variables of the model at time t and $\boldsymbol{\xi}^{\text{TSM}}(t)$ is the approximation with the TSM surrogate. Here, $\theta^{(0)}$ is the evaluation point around which the polynomial surrogate is constructed.

For an arbitrary number of parameters, all parameters are collected in the vector $\boldsymbol{\theta}$. The difference between the evaluation point $\boldsymbol{\theta}^{(0)}$ and the actual parameter set is given as $\tilde{\boldsymbol{\theta}} = \boldsymbol{\theta} - \boldsymbol{\theta}^{(0)}$. With these definitions, the TSM surrogate can be defined as

$$\boldsymbol{\xi}^{\text{TSM}}(t) = \boldsymbol{\xi}^{(0)}(t) + \sum_{i=1}^{p} \tilde{\boldsymbol{\theta}}^i \cdot \boldsymbol{\xi}^{(i)}(t). \tag{17}$$

Effectively, $\boldsymbol{\xi}^{(0)}(t), \boldsymbol{\xi}^{(1)}(t), \ldots, \boldsymbol{\xi}^{(p)}(t)$ are time-dependent basis functions that do not depend on the parameters for the evaluation. Instead, these basis functions are computed at the evaluation point $\boldsymbol{\theta}^{(0)}$. Given these basis functions, the surrogate can be evaluated for any parameter set $\boldsymbol{\theta}$ by simply evaluating the polynomial expansion. The computational cost of evaluating the surrogate is negligible compared to the cost of evaluating the forward model, as no system of equations needs to be solved. It might get noted, that for an algebraic model, the TSM surrogate equals a standard Taylor expansion.

Nevertheless, the biofilm model is given in terms of a differential equation system which complicates the derivation of the basis functions. Let us refer to the system of equations (12) - (15) as $\mathcal{G}(\dot{\boldsymbol{\phi}}, \dot{\boldsymbol{\psi}}, \boldsymbol{\phi}, \boldsymbol{\psi}, \boldsymbol{\theta}) = \mathbf{0}$. The system of equations depends on the time-dependent internal variables and their time derivatives. Equations (12) - (15) constitute an implicit system of equations.

As first step, time-dependent internal variables $\boldsymbol{\xi} = \{\boldsymbol{\phi}, \boldsymbol{\psi}\}$ are expanded in a Taylor series around the point $\boldsymbol{\theta}^{(0)}$ in the parameter space as

$$\boldsymbol{\Phi}^{\text{TSM}} = \boldsymbol{\Phi}^{(0)} + \tilde{\boldsymbol{\theta}} \cdot \boldsymbol{\Phi}^{(1)} \tag{18}$$

$$\boldsymbol{\Psi}^{\text{TSM}} = \boldsymbol{\Psi}^{(0)} + \tilde{\boldsymbol{\theta}} \cdot \boldsymbol{\Psi}^{(1)}. \tag{19}$$

Naturally, the time-derivative results as

$$\dot{\boldsymbol{\Phi}}^{\text{TSM}} = \dot{\boldsymbol{\Phi}}^{(0)} + \tilde{\boldsymbol{\theta}} \cdot \dot{\boldsymbol{\Phi}}^{(1)} \tag{20}$$

$$\dot{\boldsymbol{\Psi}}^{\text{TSM}} = \dot{\boldsymbol{\Psi}}^{(0)} + \tilde{\boldsymbol{\theta}} \cdot \dot{\boldsymbol{\Psi}}^{(1)}. \tag{21}$$

The zeroth order term of the polynomial as defined in Equation (17) is computed as

$$\{\dot{\boldsymbol{\Phi}}^{(0)}, \dot{\boldsymbol{\Psi}}^{(0)}\} = \arg\left(\mathcal{G}(\dot{\boldsymbol{\phi}}, \dot{\boldsymbol{\psi}}, \boldsymbol{\phi}, \boldsymbol{\psi}, \boldsymbol{\theta})\big|_{\boldsymbol{\theta}=\boldsymbol{\theta}^{(0)}} = \mathbf{0}\right). \tag{22}$$

Equation (22) is the solution of the original equation system at $\boldsymbol{\theta}^{(0)}$.

The derivation of the first order term is more involved. The first order term is computed by evaluating the first derivative of the system of equations with respect to the parameters at the evaluation point $\boldsymbol{\theta}^{(0)}$ as

$$\{\dot{\boldsymbol{\Phi}}^{(1)}, \dot{\boldsymbol{\Psi}}^{(1)}\} = \arg\left(\frac{\partial}{\partial \boldsymbol{\theta}} \mathcal{G}(\dot{\boldsymbol{\phi}}, \dot{\boldsymbol{\psi}}, \boldsymbol{\phi}, \boldsymbol{\psi}, \boldsymbol{\theta})\big|_{\boldsymbol{\theta}=\boldsymbol{\theta}^{(0)}} = \mathbf{0}\right). \tag{23}$$

An equation system very similar to the original system of equations is obtained. The system of equations is also non-linear and implicit. Equations (22) and (23) are solved sequentially, i.e., first the zeroth order term is computed and then the first order term is computed. In other words, the system of equations is solved in a staggered manner. Higher order terms can be found similarly.

The first order term is computed by using the Computer Algebra System Mathematica.

4 Numerical results

In this section, we present numerical results for the TSM surrogate and compare it with the forward model in terms of accuracy and computational cost. In particular, we are investigating a case with two species and the growth coefficient matrix $\boldsymbol{A} = \begin{bmatrix} 2 & 1 \\ 1 & 1 \end{bmatrix}$, the antibiotic sensitivity $b_1 = 1$ and $b_2 = 0$ and the viscosity $\eta_1 = \eta_2 = 1$. The nutrients $c^* = 10\,\mathrm{J/m^2}$ and the antibiotics $\alpha^* = 100\,\mathrm{J/m^2}$ are kept constant during the simulation. The initial conditions for the volume fractions are given as $\phi_1 = \phi_2 = 0.2$. The constant of the barrier method is set to $K_i = 10^{-4}\,\eta_i$ and $K_0 = 10^{-4}$. The evolution of the volume fractions over time is shown in Figure 1. The first species grows faster than the second species, as it has a higher growth coefficient and despite the higher sensitivity to the antibiotics. A significant interaction effect can be observed when the sum of the volume fractions of the biofilms reaches the total available volume. After this, the growth of the biofilm is significantly reduced. The second species even reduces in volume fraction until it reaches a volume of zero. This example showcases the complex interaction of the biofilms and the non-linear effects that arise from the coupling of the evolution equations and the volume constraint.

In the following, we are interested in the effect of the growth coefficients a_{ij}, the antibiotic sensitivity b_i on the evolution of the biofilm. Consequently, the parameter set is set as $\boldsymbol{\theta} = [a_{11}, a_{12}, a_{21}, a_{22}, b_1, b_2]$. We assume that all parameters are normally distributed and independent. The coefficient of variation (CoV), i.e., the fraction of standard deviation of the parameter and the mean of the parameter, is varied in the following examples.

As first case, we evaluate the relative error of the TSM surrogate compared with the forward model for different coefficients of variation. The relative error is defined as

$$\epsilon = \sum_{i=1}^{n_t} \frac{||\boldsymbol{\phi}_i - \boldsymbol{\phi}_i^{\mathrm{TSM}}||}{||\boldsymbol{\phi}_i||} \tag{24}$$

CoV	0.025	0.05	0.1	0.15	0.2	0.25	0.3
Error	0.13%	0.47%	1.7%	3.2%	5.1%	6.7%	9.3%

Table 1: Comparison of the relative error for 100 realizations.

with the total number of time steps n_t, the volume fractions ϕ_i at time step i and the volume fractions ϕ_i^{TSM} at time step i computed with the TSM surrogate. A set of 1000 realizations with different parameter values is used to compute the relative error for a given coefficients of variation. The averaged results are presented in Table 1. The relative error increases with increasing coefficient of variation, as the surrogate is most accurate in a neighborhood around the evaluation point.

To get a better understanding of the relative error value, we present the evolution of the volume fractions over time for the TSM surrogate and the forward model in Figure 2 for a single parameter set. In both cases, the coefficient of variation is set to 0.2. In Figure 3a, a relative error of 0.87% results. In Figure 3b, the relative error is 4.4%. The TSM surrogate is shown as a red dashed line and the true model is shown as a solid blue line. Differences between the TSM surrogate and the forward model mostly occur near the end of the simulation, where one of the volume fractions approaches zero. A smaller difference between the TSM surrogate and the forward model is observed near the point where the sum of the volume fractions approaches the total available volume. In both cases, the dynamic of the forward model changes significantly and a linear approximation is not sufficient. Nevertheless, for most of the simulation, the TSM surrogate captures the solution of the forward model very well despite significant differences to the solution of the forward model at the evaluation point as presented in Figure 1.

Further, we compare the evolution of the relative error over time for two different coefficients of variation in Figure 3. In total, 10000 realizations are used to compute the relative error at each time step. The relative error is averaged over all realizations. The relative error increases with increasing coefficient of variation, as the surrogate is most accurate in a neighborhood around the evaluation point. The relative error peaks at the end of the simulation, where one of the volume fractions approaches zero and when the sum of the volume fractions approaches the total available volume.

As last investigation, we compare the computational cost of evaluating the TSM surrogate and the forward model. The time to evaluate the TSM surrogate and the forward model are presented in Table 2 in case of the evaluation of 100 realizations of the parameters. In addition to the here investigated two species model, we also present the results for a four species model. The computational cost of evaluating the TSM surrogate is lower than the cost of evaluating the forward model for both cases. In fact, the computational cost of the TSM surrogate does not increase with the number of realizations, as each additional evaluation only requires the evaluation of the polynomial expansion, which is computationally negligible. In contrast, the computational cost of evaluating the forward model increases linearly with the number of realizations, as each realization requires solving a system of equations at every time

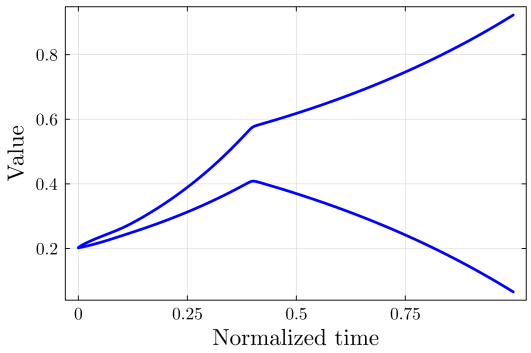

Figure 1: Evolution of volume fractions over time.

	forward model	TSM surrogate
2 species	400 ms	44 ms
4 species	1300 ms	784 ms

Table 2: Comparison of the computation time for 100 realizations.

step. For the case of the 2 species model, 5 parameters are varied, whereas for the 4 species model, all 14 parameters of the matrices $\boldsymbol{A}$ and $\boldsymbol{B}$ are varied. This explains the higher computational cost for the 4 species model compared to the 2 species model.

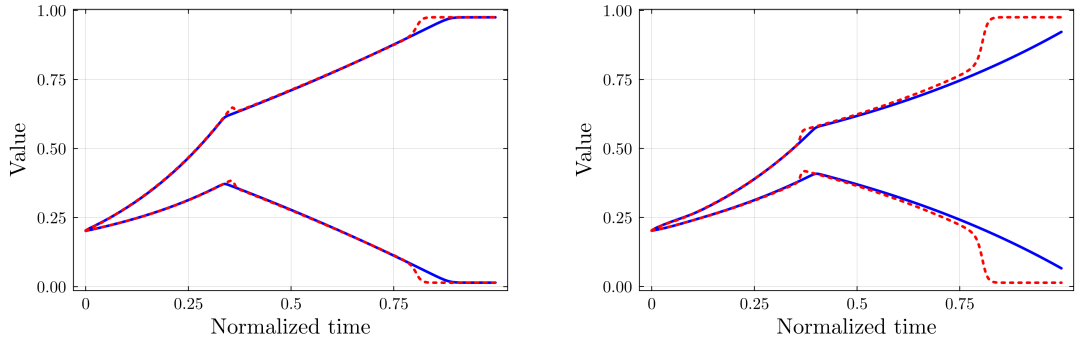

(a) Example 1

(b) Example 2

Figure 2: Evolution of volume fractions over time with the forward model in solid blue and the TSM surrogate in dashed red.

5 Conclusion

In this work, the Time-separated stochastic mechanics (TSM) is evaluated as a surrogate modeling approach for a recently developed multi-species biofilm model. The TSM surrogate is defined by derivative matching, i.e., the first p partial derivatives of

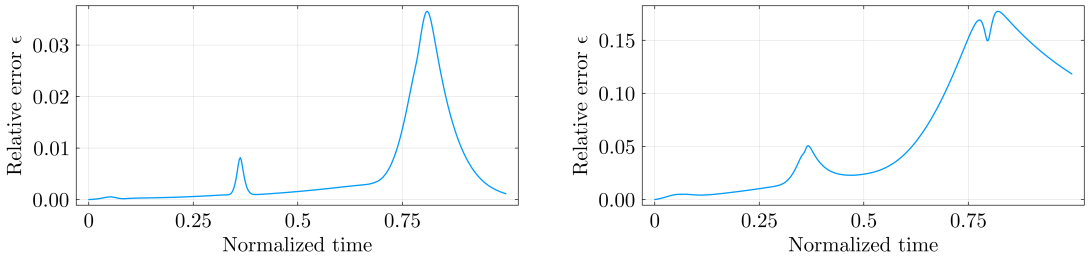

(a) CoV = 0.05 (b) CoV = 0.2

Figure 3: Evolution of relative error over time of the TSM surrogate.

the TSM-surrogate coincide with the forward model at a given point in the parameter space. The surrogate is evaluated for different coefficients of variation and compared with the forward model in terms of accuracy and computational cost. The results show that the TSM surrogate can capture the solution of the forward model very well for a wide range of parameters, while significantly reducing the computational cost compared to evaluating the forward model directly. This work is based on the papers [1] and [2].

Acknowledgements

Funded by the European Union (ERC, Gen-TSM, 101124463). Views and opinions expressed are however those of the authors only and do not necessarily reflect those of the European Union or the European Research Council Executive Agency. Neither the European Union nor the granting authority can be held responsible for them. The authors highly acknowledge the funding by the German Research Foundation (Deutsche Forschungsgemeinschaft, DFG) through the project grant SFB/TRR-298-SIIRI – Project-ID 426335750.

References

[1] F. Klempt, H. Geisler, M. Soleimani, P. Junker, “A continuum multi-species biofilm model with a novel interaction scheme“, arXiv preprint: 2509.01274.

[2] L. Fritsch, H. Geisler, J. Grashorn, F. Klempt, M. Soleimani, M. Broggi, P. Junker, M. Beer, “Bayesian Updating of constitutive parameters under hybrid uncertainties with a novel surrogate model applied to biofilms“, arXiv preprint:2512.15145.

[3] I. Klapper, J. Dockery, “Mathematical description of microbial biofilms“, SIAM Review, 52(2), 221-265, 2010.

[4] P. Marsh, ”Dental plaque: biological significance of a biofilm and community life-style”, Journal of Clinical Periodontology, 32, 7-15, 2005.

[5] C. Picioreanu, J.-U. Kreft, M. C. M. van Loosdrecht, "Particle-based multidimensional multispecies biofilm model", Applied and Environmental Microbiology, 70(5), 3024-3040, 2004.

[6] G. James, L. Beaudette, J. Costerton, "Interspecies bacterial interactions in biofilms", Journal of Industrial Microbiology and Biotechnology, 15(4):257-262, 1995.

[7] M. Chaudhry, S. Beg, "A review on the mathematical modeling of biofilm processes: advances in fundamentals of biofilm modeling", Chemical Engineering & Technology: Industrial Chemistry-Plant Equipment-Process Engineering-Biotechnology, 21(9):701-710, 1998.

[8] P. Junker, D. Balzani, "An extended Hamilton principle as unifying theory for coupled problems and dissipative microstructure evolution", Continuum Mechanics and Thermodynamics, 33(4):1931-1956, 2021.

[9] P. Wriggers, "Computational contact mechanics", Springer, 2006.

[10] H. Geisler, P. Junker, "Time-Separated Stochastic Mechanics for the Simulation of Viscoelastic Structures with Local Random Material Fluctuations", Computer Methods in Applied Mechanics and Engineering 407 (März 2023): 115916, https://doi.org/10.1016/j.cma.2023.115916.

[11] H. Geisler, C. Erdogan, J. Nagel, P. Junker, "A New Paradigm for the Efficient Inclusion of Stochasticity in Engineering Simulations: Time-Separated Stochastic Mechanics", Computational Mechanics 75, Nr. 1 (Januar 2025): 211–35, https://doi.org/10.1007/s00466-024-02500-5.